Low Temperature Physics/Fizika Nizkikh Temperatur, 2012, v. 38, No. 8, pp. 860–870

Metal atom (Zn, Cd and Mg) luminescence in solid neon

Brendan Healy, Paul Kerins, and John G. McCaffrey

Department of Chemistry, National University of Ireland - Maynooth,
Maynooth, County Kildare, Ireland
E-mail: john.mccaffrey@nuim.ie

Received March 13, 2012

Luminescence spectroscopy of the metal atoms Mg, Zn and Cd isolated in solid neon is recorded using pulsed synchrotron radiation excitation of the $ns^1np^1\ ^1P_1$–$ns^2\ ^1S_0$ resonance (n = 3, 4 and 5 respectively) transitions. Two features, a dominant band and a red-shoulder, are identified in the UV absorption spectra of Zn/Ne and Cd/Ne. Excitation of these features yields distinct emission bands with the red-shoulder absorption producing the smaller, Stokes-shifted emission. Nanosecond decaytime measurements, made with the time correlated single photon counting technique indicate the emission bands arise from the spin singlet $^1P_1 \rightarrow {}^1S_0$ transition. Hence, it is concluded the duplication of absorption and emission features in the Cd/Ne and Zn/Ne systems arises from metal atom occupancy in two distinct sites. In contrast, Mg/Ne luminescence consists of single excitation and emission bands, indicative of occupancy in just one site. The occurrence of distinct photophysical characteristics of the linewidths, Stokes shift and lifetimes in the Mg/Ne system, compared with those recorded for Zn/Ne and Cd/Ne, is rationalised in terms of a different site occupancy for atomic Mg. Accurate interaction potentials for the ground states of the M·Ne diatomics are used to analyse site occupancies and interpret this contrasting behavior.

PACS: **67.80.–s** Quantum solids;
32.70.Jz Line shapes, widths, and shifts;
32.70.Fw Absolute and relative intensities.

Keywords: luminescence spectroscopy, rare gas, MG/Ne, Zn/Ne.

1. Introduction

Several absorption studies [1] of matrix-isolated metal atoms have indicated pronounced threefold splitting on resonance $P \leftarrow S$ transitions and while magnetic circular dichroism (MCD) work [2,3] has revealed the origins of the characteristic threefold splitting is likely due to Jahn–Teller coupling in the excited P state, a fundamental obstacle precluding a conclusive assignment is lack of knowledge of the site occupied by the guest atom in the host solid. Clearly, a better understanding of the underlying physical effects contributing to the spectral behavior of these model matrix-isolated systems relies on an identification of guest site occupancy. In recent years, our Group at Maynooth has utilised luminescence spectroscopy which, having the facility to record excitation spectra for different emission bands, affords an opportunity of resolving features in the complex absorption spectra that may arise from different site occupancies.

To-date our efforts have focussed on guest metal atoms isolated in the heavier rare gases Ar, Kr and Xe. The elements chosen, Mg, Zn and Cd, provide fully allowed $ns^1np^1\ ^1P_1$–$ns^2\ ^1S_0$ transitions between the spin singlet states of these ns^2 metal atoms where n = 3, 4 and 5 respectively. A number of absorption studies [4] have been conducted for the atoms Mg [5], Zn [6] and Cd [7] isolated in the solid rare gases as host materials. The threefold splitting observed for the absorption bands of these metal atoms in the solid rare gases Ar, Kr and Xe (M/RG) has been assigned to the dynamic Jahn–Teller effect [8,9] on the assumption that the ground state metal atom is isolated in a highly symmetrical site of the solid rare gases. Excitation spectra recorded in luminescence studies confirm the existence of the threefold splitting in the Mg/RG [10], Zn/RG [11] and Cd/RG [12] systems.

While much fewer matrix studies have been done on metal atoms in solid neon [4], absorption spectra of the three metals of interest to this work have been recorded. In stark contrast to the heavier rare gases, absorption spectra of the Mg/Ne [8], Cd/Ne [12] and Zn/Ne [13–15] systems do not show clear evidence of threefold splitting. Instead the Mg/Ne system exhibits a single featureless band, Zn/Ne shows evidence for a weak red-shoulder on a main band, while Cd/Ne presents a resolved red feature close to the

main band which is featureless. Currently, luminescence spectra have only been recorded [12] for the Cd/Ne system.

The existence of only limited luminescence data for metal atoms isolated in solid neon is unfortunate, in that the much smaller site size in the neon lattice, compared with the heavier rare gases, affords an opportunity to identify the site occupancy of the metal atom. A hint of the anticipated site occupancies can be gleaned from a comparison of the substitutional site sizes of the solid rare gases and the metal atom-rare gas atom van der Waals bond lengths. The substitutional site diameter in solid neon is 3.155 Å, considerably smaller than the values of 3.756, 3.991 and 4.335 Å for the corresponding sites in the solid rare gases Ar, Kr and Xe respectively. This behavior is very different to the almost invariant ground state bond lengths of the diatomic M·RG van der Waals molecules formed between an ns^2 metal atom (M) and the rare gases (RG), neon through to xenon. For example, in the Zn($4s^2$ $^1S_0$)·RG series the van der Waals bond lengths decrease by only 0.2 Å on going from Zn·Xe to Zn·Ne, while the substitutional site diameter has decreased by almost 1.2 Å from solid xenon to solid neon. From these size considerations, the obvious candidate for atomic zinc occupancy in the heavier rare gases is a substitutional site, in which a single rare gas atom of the host solid is replaced by the guest metal atom. However, the same site occupancy for atomic zinc in neon seems unlikely.

The recent theoretical study by Gervais and co-workers [16] on the alkali metal atom series (M = Li, Na and K) isolated in solid argon has provided considerable insight into the isolation of range of guest atoms in a given matrix system. On a related subject, Fajardo has used Monte Carlo techniques on the Li/Ne [17] system to investigate the occupancy of this metal atom in a solid neon host. The results obtained indicated single substitutional sites were not occupied, but tetravacancy sites could accommodate Li atoms with only a minor disruption of the fcc lattice.

With the objective of investigating ns^2 metal atom site occupancy in neon matrices, accurate diatomic M·Ne ground state interaction potentials are clearly of vital importance. Fortunately, the ground $^1\Sigma_0$ state bond lengths of the diatomic molecules Zn·Ne [18], Mg·Ne [19] and Cd·Ne [20] are now known, having values of 4.16, 4.4 and 4.26 Å respectively. From these bond lengths, it can be seen that the metal atoms would be very "cramped", if rigid, single substitutional sites in Ne are occupied whose diameter is only 3.154 Å. A detailed account of the luminescence recorded for atomic zinc and atomic magnesium isolated in solid neon will be presented in this contribution as well as new Cd/Ne emission data.

2. Experiment

Neon samples, containing isolated atoms of Zn, Cd and Mg were prepared at HASYLAB/ DESY, Hamburg by co-depositing metal vapour with neon onto an LiF window. Samples were formed at 6 K, using a previously described liquid helium cryostat [21] capable of reaching a minimum temperature of 4 K, and then annealed to 8–9 K to minimise the loss of solid neon. Metal vapours were produced by electron bombardment using an Omicron EFM3 ultra high vacuum (UHV) evaporator. For Mg, a 1 mm diameter wire was used, while Cd and Zn vapours were generated from the metal foils coiled inside a 5 mm diameter molybdenum crucible. The metals used were all of 99.98% purity as supplied by Goodfellow Cambridge Ltd.

Synchrotron radiation produced at DESY was used as the excitation source to record luminescence spectroscopy. Steady-state emission and excitation spectra in the UV region were recorded with a 0.4 m Seya–Namioka monochromator and detected with a Hamamatsu MCP 1645U-09 microchannel plate. Transmitted light was detected by a Valvo XP2020Q photomultiplier tube. The corresponding absorption spectra were obtained using the transmittance of a pure Ne sample, recorded at the same temperature as the blank. Excited state lifetime measurements in the nanosecond range were carried out using the time correlated single photon counting (TCSPC) technique [22]. The synchrotron radiation generated from the Doris-III storage ring at HASYLAB/DESY was operated in the "5 bunch mode" with a narrow temporal pulse width (full width at half maximum 120 ps) at a repetition rate of 5.208 MHz. At this high excitation frequency, the longest lifetimes which can be measured with the TCSPC technique is 1 μs. Emission decay times were extracted using the ZFIT [23] program by fitting trial functions, convoluted with the temporal profile of the excitation pulse, to the recorded decay curves.

3. Results

3.1. M/Ne *absorption*

Absorption spectra were used to monitor the extent of atomic isolation in the M/Ne (M = Zn, Cd and Mg) matrices formed. As indicated in the bottom trace of Fig. 1, small metal flux (< 0.5 nA) is required to produce Zn/Ne samples consisting predominantly of isolated atoms. Increasing the flux leads to the formation of samples containing, as shown by the upper trace in Fig. 1 a range of metal clusters but especially zinc dimer. The absorption spectra recorded for the lowest concentration Zn/Ne, Cd/Ne and Mg/Ne matrix samples are presented in Fig. 2 along with their fully allowed singlet $^1P_1$–$^1S_0$ gas phase transitions.

3.2. Zn/Ne *emission*

A summary of the luminescence spectroscopy recorded at 4.1 K for the lowest concentration Zn/Ne samples is presented in Fig. 3. The emission spectrum produced with excitation of the dominant absorption, centred at approximately at 205.4 nm, consists of a single band located at 212.8 nm. The excitation spectrum recorded monitoring this emission wavelength is centred at 206 nm but evidently contains at least two features. This excitation profile is

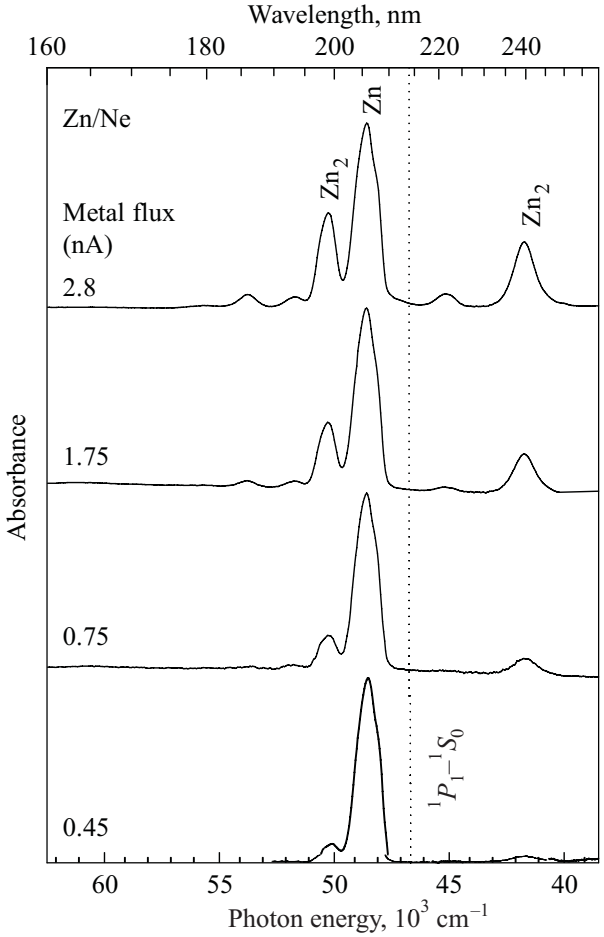

Fig. 1. A concentration study of the isolation of Zn in neon matrices formed at 4.1 K as monitored with absorption spectroscopy. The dominant absorption band in the sample formed with the lowest metal flux (presented in the bottom trace) corresponds to atomic zinc. This structured band is located to the blue of the gas phase atomic $4s^1 4p^1\ {}^1P_1$–$4s^2\ {}^1S_0$ transition but shows signs of an unresolved red shoulder. Increasing the metal flux allows identification of the features at 241 and 199 nm as arising from zinc dimer.

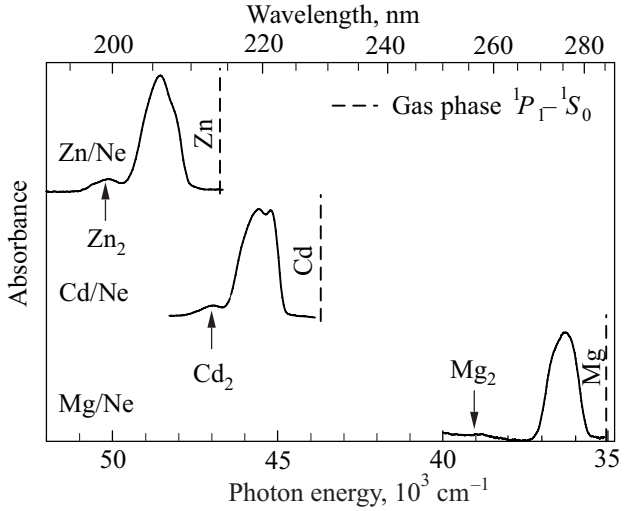

Fig. 2. A summary of the absorption bands recorded for the three metals Zn, Cd and Mg isolated in solid Ne. Concentration studies, such as that presented in Fig. 1, allow the indicated dimer and atomic attributions to be made for the observed bands. The atomic absorptions are blue-shifted from their associated gas phase $^1P_1$– $^1S_0$ transitions whose locations are shown by the dashed vertical lines. A comparison of the atomic absorption bands recorded in three M/Ne systems reveals the simplest structure in the Mg/Ne system.

entirely consistent with the absorption band scanned at 4.1 K (see Fig. 2) showing signs that it consists of two features. The main feature is centered at 205.4 nm with a weaker red-shoulder located at 207.8 nm. A comparison of the emission profile recorded with excitation of the weaker 207.8 nm feature is shown in the upper panel of Fig. 4. The resulting emission at 212.0 nm is broader than the dominant band centered at 212.7 nm and is blue-shifted slightly.

The locations of the features making up the multicomponent Zn/Ne excitation profiles were extracted by fitting [24] the recorded bands with Gaussian functions. Figure 5 displays the best fits obtained for the absorption and emission bands. The locations of the features extracted in the fits conducted are listed in the figure caption. As shown on the left in Fig. 5, a minimum of four Gaussian functions was required to provide an acceptable fit of the absorption profile. In contrast, the emission band produced with excitation at 205.4 nm is made up of just a single component.

The temporal decay curve recorded with the TCSPC technique for the 212.8 nm emission band is shown on an 8 ns range in the inset of Fig. 3. Single exponential fits

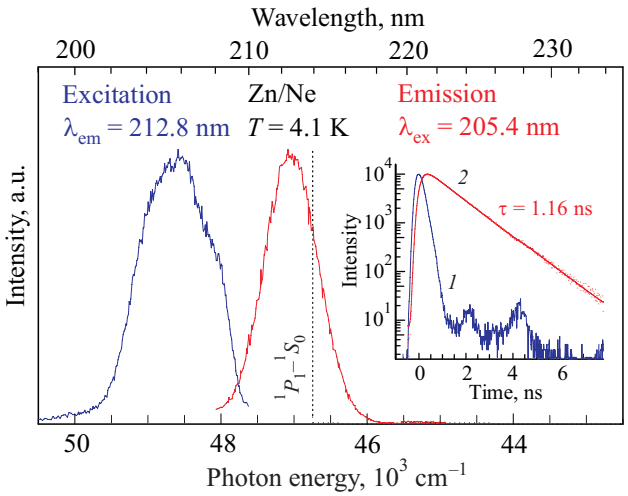

Fig. 3. (Color online) Excitation and emission spectra recorded at 4.1 K in the Zn/Ne system after annealing to 8 K. As indicated, both excitation and emission are located to the blue of the gas phase atomic Zn $4s^1 4p^1\ {}^1P_1$–$4s^2\ {}^1S_0$ transition, represented by the vertical dotted line. The inset shows a semi-log plot of the 213 nm emission decay curve, depicted by red dots, recorded with the TCSPC technique and generated from excitation at 205 nm. The blue curve (*1*) centred at $t = 0$ is the temporal profile of the synchrotron radiation pulse. A single exponential function fit of the emission decay curve is depicted by the solid red line (*2*), yielding a lifetime of 1.16 ns.

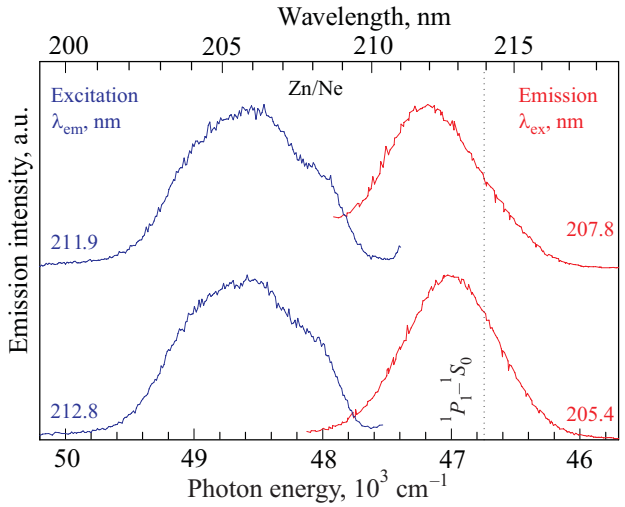

Fig. 4. (Color online) A summary plot of all the excitation and emission features recorded at a temperature of 4.1 K for the $4s^1 4p^1\ ^1P_1$–$4s^2\ ^1S_0$ transition of atomic Zn isolated in solid Ne. The lower panel denotes excitation and emission recorded from the dominant excitation feature, while the upper panel shows the luminescence recorded for the weaker red-shoulder in the excitation profile. The location of the $^1P_1$–$^1S_0$ transition of atomic Zn in the gas phase is depicted by the vertical dotted line.

carried out on the emission decay curves yielded a decay time of 1.16 ns for this band. The 212.0 nm emission decay curve also only needed a single exponential fit, but its decay time was slightly shorter, having a value of 1.10 ns. These values were observed to be temperature independent and are therefore identified as the radiative lifetimes. Since the gas phase [26] lifetime of the $4s^1 4p^1\ ^1P_1$–$4s^2\ ^1S_0$ transition is known to be 1.41 ns and the fact the solid state luminescence profiles are in the vicinity of this transition, it can stated with confidence the observed emission features arise from the excited singlet $4s^1 4p^1\ ^1P_1$ state of atomic zinc. As Fig. 3 clearly indicates, the excitation and emission profiles of Zn/Ne are both shifted to the blue of the gas phase transition [25] at 213.86 nm.

3.3. Mg/Ne *emission*

A summary of the luminescence recorded in the Mg/Ne system is presented in Fig. 6. From the location of the free atomic $3s^1 3p^1\ ^1P_1$–$3s^2\ ^1S_0$ transition, it can be seen that the Mg/Ne matrix excitation feature is shifted to the blue, by about the same amount that the emission feature is shifted to the red of the gas phase position. No changes were noted in the luminescence (excitation or emission) features on scanning after annealing to 8 K. Thus, there is no evidence of thermally unstable sites in Mg/Ne samples deposited at 6 K.

The results of Gaussian fits are shown in Fig. 7 indicating that the absorption band in Mg/Ne contains three components, whose locations and bandwidths are provided in

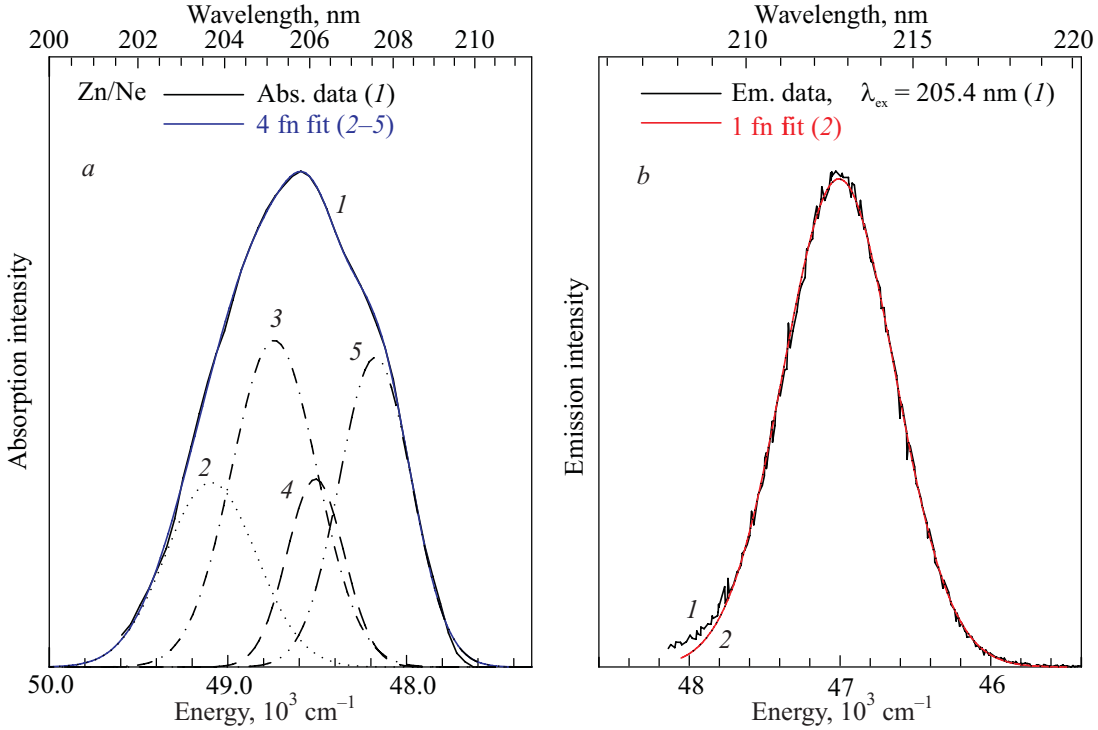

Fig. 5. (Color online) Lineshape analyses of the absorption (*a*) and emission (*b*) spectra of Zn/Ne. Four Gaussian functions were required to provide a reasonable fit to the absorption profiles while only one is needed to fit the emission. The three features extracted in the blue absorption profile are located at 49095, 48740 and 48509 cm^{-1} (203.68, 205.17 and 206.15 nm) with bandwidths of 600, 561 and 375 cm^{-1} respectively. The red excitation component is centred at 48175 cm^{-1} (207.57 nm) having a width of 472 cm^{-1}. The quoted bandwidths are all fwhm values calculated as $\Delta = s^*\sqrt{[8\ \ln(2)]}$ where s is the variance in the fitted Gaussian function, $G(x) = a\ \exp[-(x-m)^2/(2s^2)]$. A fit of the emission yielded a band centred at 47006 cm^{-1} (212.73 nm) and a width of 872 cm^{-1}.

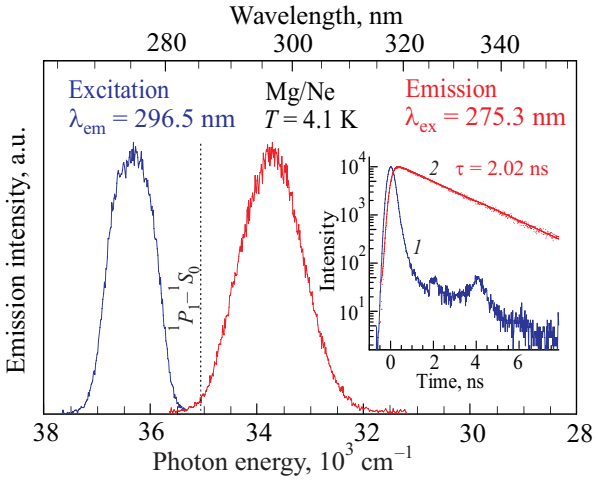

Fig. 6. (Color online) Excitation and emission spectra recorded at 4.1 K in the Mg/Ne system after annealing to 8 K. The location of the Mg atom gas phase $3s^1 3p^1\ ^1P_1$–$3s^2\ ^1S_0$ transition is represented by the vertical dotted line. Shown inset is a semi-log plot of the 296.5 nm emission (red dots) generated from excitation at 275 nm. The blue trace (*1*) centred at $t = 0$ is the temporal profile of the synchrotron radiation pulse. A single exponential fit of the decay curve, depicted by the solid red line (*2*), reveals a decay time of 2.02 ns.

the figure caption. Exciting into the three absorption wavelengths, 272, 275 and 278 nm resulted in identical emission ands centred at 296.5 nm. This emission band could, as shown on the right hand panel in Fig. 7, be satisfactorally fit with a single function.

The inset of Fig. 6 presents the temporal characteristics of the Mg/Ne 296.5 nm emission band. An acceptable fit is shown by the solid line passing through the recorded decay curve represented by the dots, while the blue curve, centred at $t = 0$, depicts the time structure of the synchrotron radiation. The emission decay curve was fit using a single exponential function, with a decay time of 2.02 ns. This decay time did not change upon recording the emission decay profiles at higher temperatures, and is thereby identified as the radiative lifetime. Moreover, the decay time of the 296.5 emission did not change with excitation of the three absorption components. Since the gas phase $3s^1 3p^1\ ^1P_1$–$3s^2\ ^1S_0$ transition of atomic magnesium [25] occurs at 285.21 nm with a lifetime [26] of 2.02 ns, the Mg/Ne emission centered at 296.5 nm clearly originates from the excited $^1P_1$ state of the Mg atom.

3.4. Cd/Ne *emission*

A new emission feature has been identified in Cd/Ne since the original data was first published [12]. It is shown in the upper panel of Fig. 8 and was produced by excitation of the component furthest to the red in the Cd/Ne absorp-

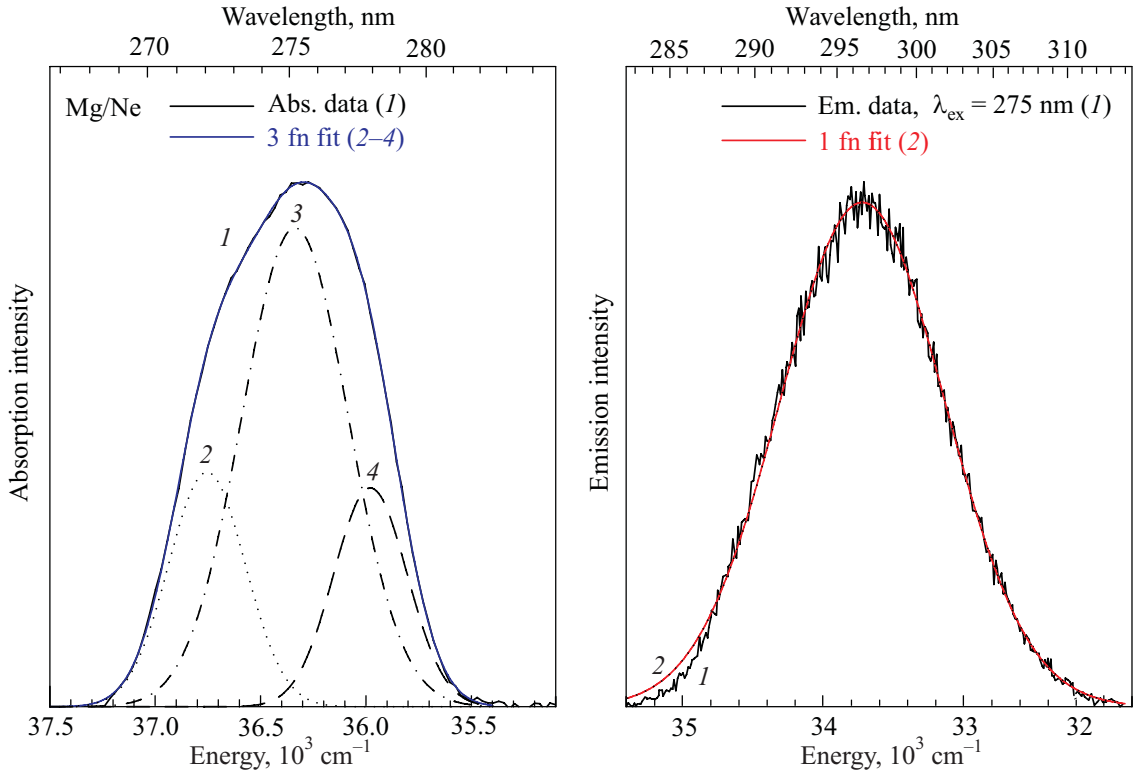

Fig. 7. (Color online) Lineshape analyses of the Mg/Ne absorption and emission profiles done with Gaussian functions to resolve the components present. The absorption band consists of only three components located at 36755, 36336 and 35979 cm^{-1} (272.07, 275.21, 277.94 nm) with bandwidths of 429, 595, 411 cm^{-1} respectively. The emission fit, shown on the right, yielded corresponding values of 33718 cm^{-1} (296.57 nm) and a width of 1380 cm^{-1}.

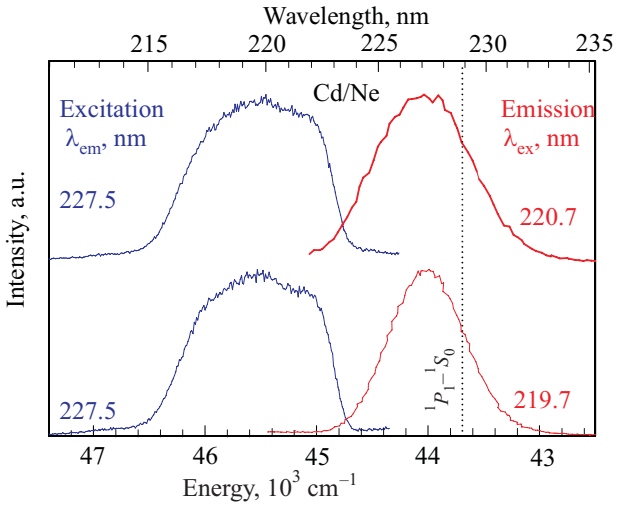

Fig. 8. (Color online) A composite plot of the two excitation and emission features that arise for the Cd/Ne $5s^15p\ ^1P_1$–$5s^2\ ^1S_0$ transition, recorded at a temperature of 4.5 K. The lower panel denotes emission recorded from the dominant feature in the excitation profile. The Cd gas phase $^1P_1$–$^1S_0$ transition is portrayed by the dotted line.

tion feature (see Fig. 2). The new emission band [27] centred at 226.9 nm, exhibits a small blue shift with respect to the previously recorded emission [12] band at 227.3 nm. Fits of the recorded emission decay curves of the 227.3 nm band revealed the presence of a risetime in addition to a 1.27 ns decay time. The gas phase [26] lifetime is known to be 1.89 ns, while the radiative lifetime [12] of the 227.3 nm emission of Cd/Ne has a shorter value of 1.27 ns.

A comparison of the site-dependent excitation and emission bands recorded for the $5s^15p^1\ ^1P_1$– $5s^2\ ^1S_0$ transition of atomic Cd isolated in Ne is presented in Fig. 8. The excitation and emission profiles in this system are, as in the Zn/Ne system, both shifted to the blue of the gas phase transition. Indeed as seen in the Zn/Ne system, the excitation profile displays distinct signs that it consists of multiple components. A lineshape analysis was used to extract these components. Double and triple Gaussian functions fits to the absorption (or excitation) profiles were not successful. However, fitting the absorption band with four Gaussian functions proved, as illustrated in Fig. 9, to be acceptable. In contrast, the emission band centered at 227.3 nm was easily fit to a single Gaussian function as displayed on the right in Fig. 9. Details of the values extracted in these fits are given in the figure caption. Thus the dominant feature at 219.7 nm in the Cd/Ne absorption profile, consists of three components, while the resolved red feature at 222 nm appears to just be a single component.

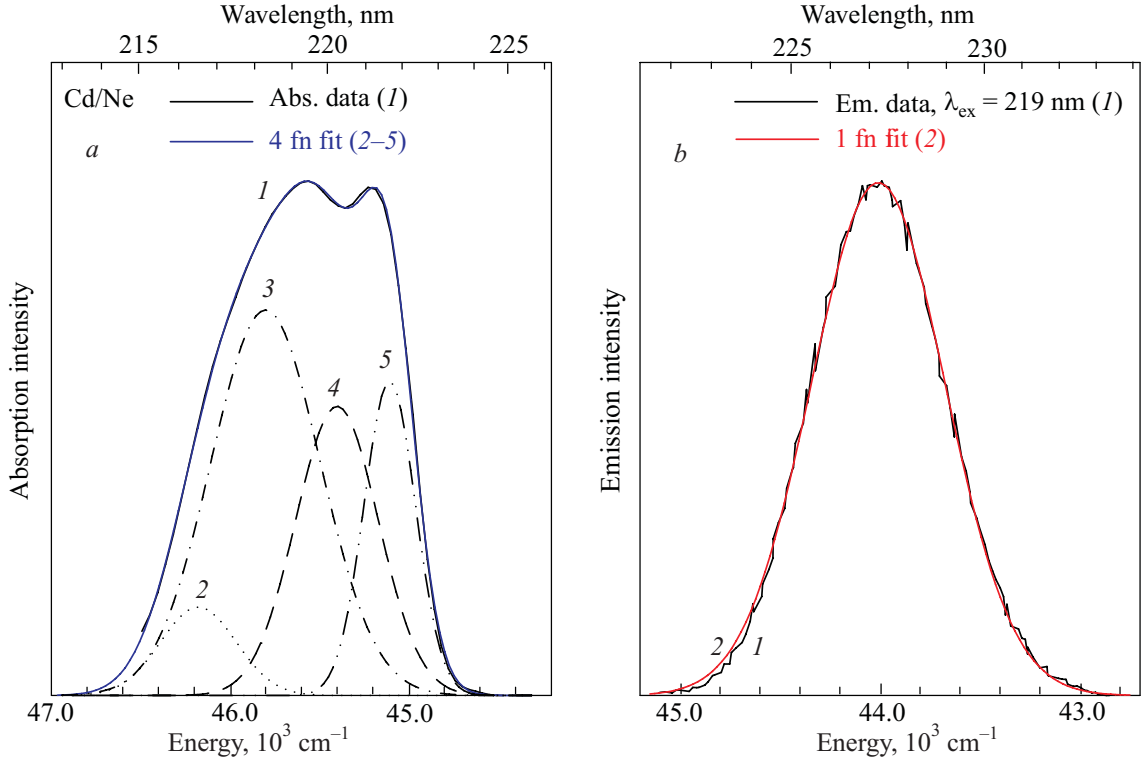

Fig. 9. (Color online) Lineshape analyses of the Cd/Ne absorption (*a*) and emission (*b*) profiles recorded at 4.5 K. Four Gaussian functions were needed to provide an acceptable fit for the absorption profile while the emission profile was readily fit with a single Gaussian function. The three components in the blue portion of the absorption band are located at 46177, 45800 and 45400 cm^{-1} (216.55, 218.34, 220.26 nm) with bandwidths of 499, 720, 544 cm^{-1} respectively. The red excitation component is centered at 45105 cm^{-1} (221.70 nm) having a width is 340 cm^{-1}. The emission fit, shown on the right, yielded corresponding values of 44008 cm^{-1} (227.23 nm) and a width of 790 cm^{-1} (*b*).

4. Discussion

4.1. M/Ne *luminescence*

Differences in the luminescence of the matrix-isolated metal atom systems Mg/Ne, Cd/Ne and Zn/Ne are highlighted in Fig. 10, in which the matrix excitation and emission bands are shown with respect to the energies of their gas phase $^1P_1$–$^1S_0$ transitions. Most striking in Fig. 10 is the very similar shifting of the excitation and emission profiles in the Zn/Ne and Cd/Ne systems and the dissimilarity of the Mg/Ne system. Thus the Zn/Ne and Cd/Ne systems both have their excitation bands shifted to the blue of the gas phase by about the same amount. Furthermore, both have their emission bands blue shifted from the gas phase — again by a similar amount. In contrast, the excitation and emission profiles in the Mg/Ne system straddle the gas phase transition, i.e., the excitation is blue-shifted to the same extent that the emission is red-shifted.

Figure 10 further illustrates how similar the excitation profiles are in the Zn/Ne and Cd/Ne systems in that both consist of a dominant band with a weaker red-shoulder. In contrast, the excitation spectrum in Mg/Ne presents a single feature blue-shifted from the gas phase transition by the same amount as the red-shoulder in the Zn/Ne and Cd/Ne excitation bands. Two other distinguishing characteristics of the Mg/Ne emission made evident in Fig. 10 are, (1) the considerably broader bandwidth, and (2) the larger Stokes shift than in the Zn/Ne or Cd/Ne systems. Possible reasons for these properties (see Table 1 for values) can be identified from a consideration of the site occupancies of the metal atoms Mg, Zn and Cd in solid neon. To do this, the van der Waals bond lengths of the metal atom neon (M·Ne) complexes will now be utilised.

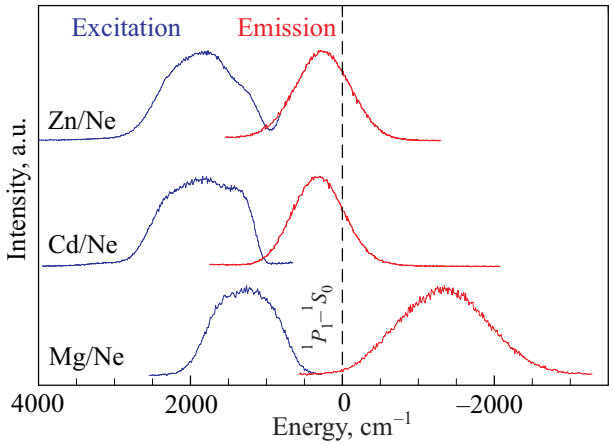

Fig. 10. (Color online) An expanded presentation of the excitation / emission bands recorded for atomic Zn, Cd and Mg isolated in solid Ne highlighting the similarities of the Zn/Ne and Cd/Ne systems and the dissimilarity of Mg/Ne. For the purposes of comparison, all the features shown have been "zeroed" with respect to their respective $np\ ^1P_1$–$ns\ ^1S_0$ gas phase transitions. Particularly evident is the similar behavior of the Zn/Ne and Cd/Ne systems whose bands are all to the blue of the gas phase atomic transition. In contrast, the matrix bands in Mg/Ne straddle the gas phase transition. Noteworthy also in Mg/Ne are the much greater bandwidth of the emission and simple excitation band which contrasts with the complex structures recorded in both Zn/Ne and Cd/Ne.

Table 1. Excitation and emission band positions, bandwidths (fwhm) and Stokes Shift pertaining to the $ns^1np^1\ ^1P_1$–$ns^2\ ^1S_0$ transition for the M/Ne solids. The gas phase positions [25] of these transitions are at 46745.413, 43692.384 and 35051.264 cm^{-1} for Zn, Cd and Mg respectively. All the matrix energies quoted are in wavenumber (cm^{-1}) units. The positions and bandwidths quoted for the matrix features in Zn, Cd and Mg were extracted in the Gaussian lineshape fits presented in Figs. 5, 7 and 9, respectively.

M/Ne	Excitation energy	Emission energy	τ_{obs}, ns	τ_{gas}, ns	Emission bandwidth	Stokes shift
Zn	48740	47006	1.15	1.41	872	1734
	48175	47192	–	–	953	1005
Cd	45800	44008	1.26	1.81	790	1792
	45105	44072	–	–	890	1033
Mg	36336	33718	2.03	2.02	1380	2597
	–	–	–	–	–	–

4.2. M·Ne *potentials*

Considering that the Zn·Ne and Cd·Ne ground $^1\Sigma_0$ state bond lengths, 4.16 and 4.26 Å respectively, are appreciably shorter than the 4.4 Å value in Mg·Ne, there is a greater likelihood that zinc and cadmium atoms will fit into a smaller site of solid neon than would a magnesium atom. To explore this further, the M·Ne ground state potentials are plotted with that of Ne_2 in Fig. 11. From the mismatch of the equilibrium bond lengths of the M·Ne diatomics and Ne_2, this comparison immediately indicates that single vacancy (sv) substitutional site occupancy is highly unfavoured in all three cases. Superimposed on the M·Ne diatomic potentials shown in Fig. 11, are the sizes of the next largest cubic sites [28] of neon, namely the tetra-vacancy (tv) and the hexa-vacancy (hv) sites. In this comparison it is evident that the nearest neighbour M–Ne distances in the tv and hv sites are located in the bound portion of the potentials for both Zn/Ne and Cd/Ne. In contrast, only the hv site occurs in this region for Mg/Ne.

This difference may explain why only a single site, possibly a hexa-vacancy, is present in the Mg/Ne system while pairs of thermally sites occur for both Zn/Ne and Cd/Ne. Thus if one adopts a large hv site assignment in Mg/Ne, the fact that the red features in the excitation profiles of Zn/Ne and Cd/Ne are situated directly in line with the excitation profile of Mg/Ne (see Fig. 10), would suggest partial

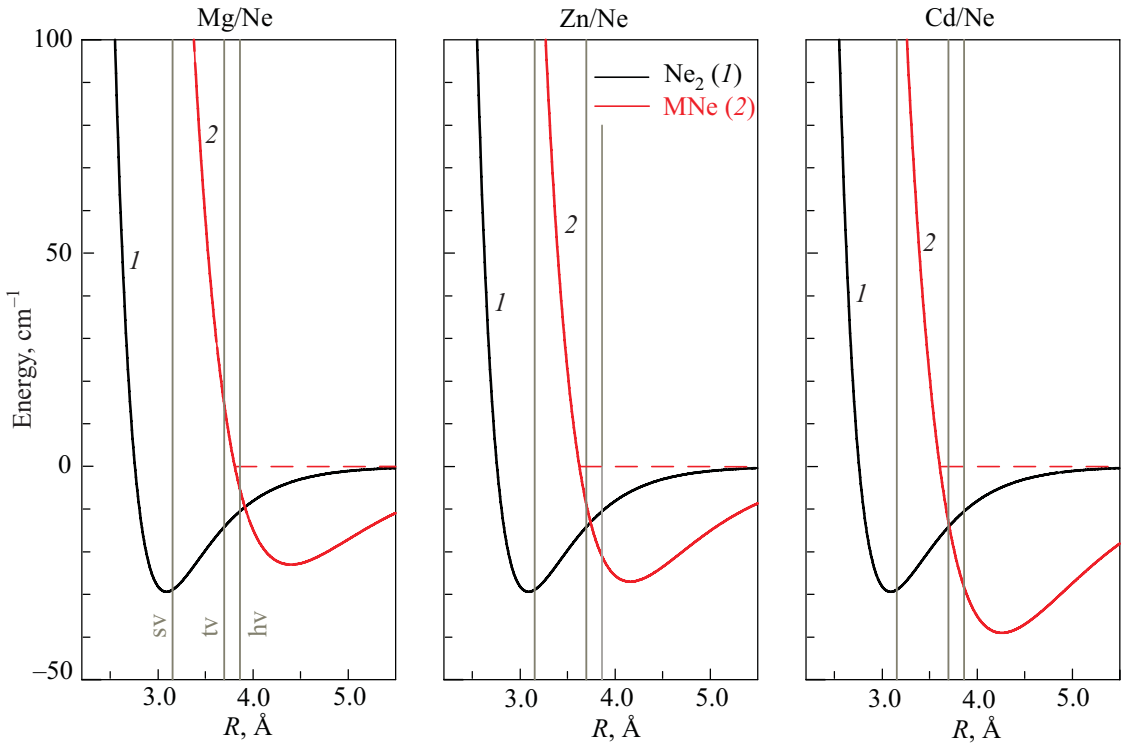

Fig. 11. (Color online) A comparison of the potential energy curve of Ne dimer with the ground state $X^1\Sigma$ state potentials for the diatomics Zn·Ne, Mg·Ne and Cd·Ne. The curves shown were generated with the data provided in Table 2. It is immediately evident that the bond lengths of the metal-neon diatomics are much greater than Ne dimer, an indication that substitutional site occupancy will be improbable for all three metal atoms in solid Ne. The size if this single vacancy (sv) site and the larger tetravacancy (tv) and hexavacancy (hv) sites are compared with the M·Ne potentials. This comparison reveals that the two larger sites have M–Ne distances on the bound portion of the Zn·Ne and Cd·Ne potentials, while only the largest hv site is in the bound portion of the Mg·Ne $X^1\Sigma$ state potential.

hexavacancy occupancy of Zn and Cd metal atoms in neon. It might be further proposed that the blue, three-component feature of Zn/Ne, centered at 204.5 nm, and the corresponding Cd/Ne feature centered at 219, arise from occupancy in a more compact tetra-vacancy site. Molecular dynamics calculations, such as those conducted on the matrix-isolated alkali metal atoms [29], are required to examine these site occupancy proposals.

Table 2. The molecular constants used to generate the potential energy curves for neon dimer and the ground X $^1\Sigma$ state of the diatomic M·Ne complexes of relevance to the isolation of atomic Mg, Zn and Cd in solid neon matrices. The Morse function is used to represent the X state potentials of all four diatomics. Data for Zn·Ne is that quoted in Ref. 18, Mg·Ne from Ref. 19 and Cd·Ne is from Ref. 20

Diatomic	D_e, cm^{-1}	ω_e, cm^{-1}	R_e, Å	β, (Å^{-1})*
NeNe	29.36745	(29.1)	3.091	2.0906[a]
MgNe($X^1\Sigma$)	23.0	14.0	4.40	1.173880
ZnNe ($X^1\Sigma$)	27.0	12.0	4.16	1.09752[b]
CdNe ($X^1\Sigma$)	39.0	13.2	4.26	1.062891

Comment: *The β coefficient was calculated with the relationship (Å^{-1}) using μ (amu) values of 9.996219, 10.903751, 15.229688 and 17.05263 for $^{20}Ne^{20}Ne$, $^{24}Mg^{20}Ne$, $^{64}Zn^{20}Ne$ and $^{116}Cd^{20}Ne$, respectively. [a]The β coefficient was obtained by fitting a Morse function to the short range (r < 4.6 Å) form of Aziz and Slaman's empirical HFD-B potential given in Ref. 33 for Ne_2. [b]The calculation involves the lower limit given in Ref. 8 for the fundamental vibrational frequency, ω_e = 12 cm^{-1}.

4.3. Zn/RG *luminescence*

The luminescence features recorded for the complete zinc/rare gas matrix series (Zn/RG) are presented together in Fig. 12. In this figure it evident that the luminescence characteristics in the Zn/Ne system are quite different to all the other Zn/RG matrix systems. The most obvious difference is that the emission in neon consists of just a single band while pairs of bands are present in the heavier rare gases. The existence of the pairs of emission bands has been attributed [30] to distinct relaxed excited state geometries originating from single vacancy site occupancy. The contrasting behaviour observed for atomic zinc in neon would suggest that the site occupied in this host is different to the other rare gases. It is also evident in Fig. 12 that the excitation band in neon is shifted furthest to the blue of the gas phase $^1P_1$–$^1S_0$ transition relative to the other Zn/RG excitation bands. However, upon closer inspection it is clear that the shift between Zn/Ne and Zn/Ar is much smaller than the linear polarisability [7] dependence that

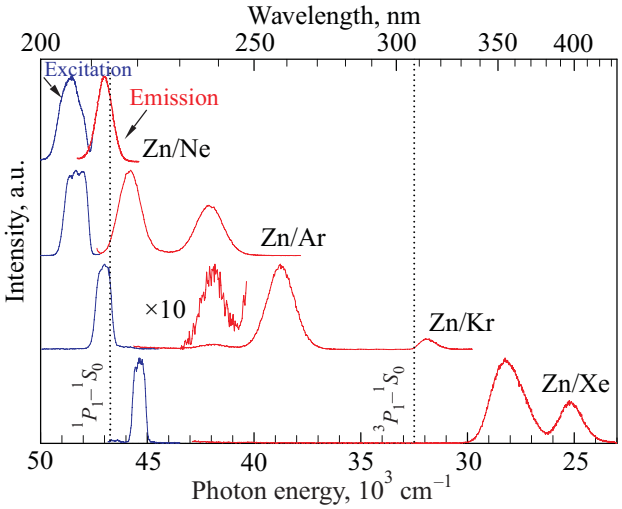

Fig. 12. (Color online) A summary of the excitation and emission spectra recorded at 4.5 K for Zn atoms isolated in the solid rare gases. The Zn/RG samples were annealed to 8.9, 33, 45 and 65 K for Ne, Ar, Kr and Xe, respectively. The atomic Zn $4p^1P_1$–$4s^1S_0$ and $4p^3P_1$–$4s^1S_0$ gas phase transitions are identified by the vertical dotted line for comparison.

exists from Zn/Ar to Zn/Xe. This behaviour points to a different site occupancy of atomic zinc in solid neon than in the rest of the rare gas hosts.

Again in contrast to atomic zinc isolated in the other rare gas solids, whose absorption bands all exhibit resolved threefold splitting, this structure is not evident in the Zn/Ne profile shown in Figs. 2 and 4. Threefold splitting is attributed to dynamic Jahn–Teller coupling [8] in the excited $^1P_1$ state resulting in the removal of the degeneracy which exists when the metal atom occupies a high symmetry site in the ground state. The highest symmetry site available to a spherical guest metal atom in an fcc lattice is a single substitutional site of cubo-octahedral symmetry. However, as indicated in Fig. 11, this site is not available for atomic zinc in neon. Even for a "large" metal atom, occupancy in a tetravacancy site of tetrahedral symmetry will still have *p*-orbital degeneracy, indicating the possibility of Jahn–Teller activity but perhaps with less pronounced manifestations than in the more compact surroundings of a cubo-octahedral substitutional site.

Indeed, a lineshape analysis allowed us to identify that three features are present in the absorption/excitation profiles of Zn/Ne even when the anticipated threefold splitting is not evident. Thus two features are readily visible in Fig. 5, yet the lineshape analysis indicates the profile is made up of four components. The three "blue" components give rise to the dominant absorption feature at 205.4 nm. The other component produces the red-shoulder feature at 207.8 nm, see Table 1. Given that these two wavelengths produce emission at different wavelengths and with different lifetimes (see Table 1 for values), the two features are spectrally distinct. On this basis it is concluded that the two components arise from different site occupancies and that the blue component has unresolved structure, consistent with Jahn–Teller interaction.

4.4. M/RG *luminescence*

The excitation and emission spectra recorded for atomic cadmium in the entire rare gas series (Ne–Xe) have been published [12] and exhibit a striking similarity to the Zn/RG series shown in Fig. 12. The key points of similarity in the Zn/RG and Cd/RG systems are as follows:

(1) The propensity of these systems to have pairs of emission bands. Thus all the Zn/RG and Cd/RG systems except Zn/Ne, Cd/Ne and Cd/Ar have pairs of bands.

(2) An increasing Stokes shift in the singlet emission bands in the series Ne, Ar and Kr. Specifically, values of 1655, 2654 and 5327 cm^{-1} are recorded for the Zn/RG (RG = Ne, Ar and Kr) series while the values are 1486, 2519 and 2742 cm^{-1} in the corresponding Cd/RG series.

The dissimilarity of the Mg/RG series [31] with both the zinc and cadmium systems can be summarised as follows. In contrast to the pairs of bands in the Zn/RG and Cd/RG systems, single emission bands are observed in all the Mg/RG [32] systems. In addition, this matrix series does not follow the photophysical trends present in the Zn/RG and Cd/RG systems. The variation of the Stokes shifts in the Mg/RG series is quite irregular with values of 2597, 2016, 1665 and 7346 cm^{-1} in solid neon, argon, krypton and xenon respectively. Another rather conspicuous but related feature of the Mg/Ne emission band, is its large bandwidth — 1406 cm^{-1} compared with values of 700 and 790 cm^{-1} in the Mg/Ar and Mg/Kr systems. The only other emission band having a bandwidth comparable in magnitude to that of Mg/Ne is the 460 nm band in Mg/Xe with a value of 1500 cm^{-1}.

4.5. M/Ne *lifetimes*

Another noteworthy feature of the Mg/Ne matrix system is the different lifetime behaviour it exhibits compared with those of the Zn/Ne and Cd/Ne systems. Thus in the Mg/Ne system the recorded matrix lifetime is almost identical to the gas phase value. This contrasts with the more usual situation in which the solid state lifetime is, as exhibited in the Zn/Ne and Cd/Ne systems, appreciably shorter than in the gas phase — see Table 1 for values. The difference between the gas and solid state lifetimes arises because of the electric field present in the host solid. However, as neon is used as the host solid in all the M/Ne systems being compared here, the lifetime differences clearly are not occurring because of differences in the dielectric constant. Rather it may arise because of differences in the local field experienced by the metal atoms, which depends on the volumes of the sites the guest atoms occupy in solid neon. The almost identical gas phase and neon

lifetimes of atomic magnesium signals the likelihood of Mg occupancy in a larger site in neon compared to the sites occupied by Cd and Zn in neon.

5. Conclusions

The Mg/Ne and Zn/Ne luminescence data reported in this study completes the rare gas series for matrix-isolated atomic Mg [10] and Zn [11], allowing a full comparison to be made with the Cd/RG solids previously analysed. The irregular shifting of the excitation features in M/Ne compared with the other members in the M/RG series, illustrated in Fig. 12 by Zn/RG, highlights the inadequacy of simple polarisability models [7] in accounting for the optical transitions in the solid rare gases. This behavior points to occupancy of the guest metal atom in a different site in neon. Furthermore, the very different behavior of Mg in neon compared with the two other ns^2 metal atoms is attributed to different ground state site occupancies of the Mg system compared with Zn and Cd. Using the known M·Ne ground state potentials, smaller tetravacancy sites are proposed for Zn and Cd — while hexavacancy is proposed for Mg. The broad width of the Mg/Ne emission is attributed to the steeply rising Mg·Ne ground state potential which exists even in this larger hv site. Solid neon matrices have been found to be ideal hosts for atomic isolation in so far as the samples formed at 6 K, exhibit no signs of metal atom occupancy in thermally unstable sites. The heavier rare gases require annealing to remove such sites.

Acknowledgements

We would like to acknowledge Dr. Peter Gürtler and Dr. Sven Petersen for technical assistance during the course of this work. This research was funded in part by the European Union, TMR, "Access to Large Scale Facilities" Programme and by the Irish Government *Forbairt* Basic Science research scheme to whom BH also gratefully acknowledges receipt of a Ph.D studentship.

1. D.M. Gruen, *Cryochemistry,* M. Moskovits and G.A. Ozin (eds.), Wiley, NY (1976) Ch. 10 and references therein to earlier work.
2. M. Vala, K. Zeringue, J. ShaksEmampour, J.C. Rivoal, and R. Pyzalski, *J. Chem. Phys.* **80**, 2401 (1984) and references therein to earlier work
3. J. Rose, D. Smith, B.E. Williamson, P.N. Schatz, and M.C.M. O'Brien, *J. Phys. Chem.* **90**, 2608 (1986) and references therein to earlier work.
4. C. Crepin-Gilbert and A. Tramer, *Intl. Rev. Phys. Chem*. **18**, 485 (1999).
5. O. Schnepp, *J. Phys. Chem. Solids* **17**, 188 (1961).
6. W.W. Duley, *Proc. Phys. Soc.* **91**, 976 (1967); *Nature* **210**, 264 (1966).
7. S.L. Laursen and H.E. Cartland, *J. Chem. Phys.* **95**, 4751 (1991).
8. R.L. Mowery, J.C. Miller, E.R. Krauz, P.N. Schatz, S.M. Jacobs, and L. Andrews, *J. Chem. Phys*. **70**, 3920 (1979).
9. M.C.M. O'Brien, *J. Chem. Phys*. **82**, 3870 (1985).
10. J.G. McCaffrey and G.A Ozin, *J. Chem. Phys*. **101**, 10354 (1994).
11. V.A. Bracken, P. Gürtler, and J.G. McCaffrey, *J. Chem. Phys*. **107**, 5290 (1997).
12. B. Healy and J.G. McCaffrey, *J. Chem. Phys*. **110**, 3903 (1999).
13. W. Schroeder, H. Wiggenhauser, W. Schrittenlacher, and D. M. Kolb, *J. Chem. Phys*. **86**, 1147 (1987).
14. Luminescence spectroscopy has been recorded by Kolb and co-workers, Ref. 13, on Zn clusters in Ne. However, in the Kolb work no atomic emission was reported for Ne samples known, from their absorption spectra, to contain Zn atoms. The reason for the previously reported non-fluorescence of atomic Zn in Ne is not clear when emission from Zn clusters was observed in these samples. However, experimental work done on atomic zinc isolated in neat N_2 samples and Ar samples doped with N_2 indicates that atomic $^1P_1$ emission is quenched very efficiently by the presence of very small amounts of molecular nitrogen. The quenching mechanism has been investigated by *ab initio* calculations (Ref. 15) and identified as an electronic-to-vibrational energy transfer process, mediated by a strongly attractive charge-transfer complex formed between the excited Zn($^1P_1$) state and N_2.
15. F. Colmenares, O. Novaro, and J.G. McCaffrey, *J. Chem. Phys.* **114**, 9911 (2001).
16. E. Jacquet, D. Zanuttini, J. Douady, E. Giglio, and B. Gervais, *J. Chem. Phys*. **135**, 174503 (2011).
17. M.E. Fajardo, *J. Chem. Phys*. **98**, 110 (1993); *ibid*. **98**, 119 (1993).
18. J.G. McCaffrey, D. Bellert, A.W.K. Leung, and W.H. Breckenridge, *Chem. Phys. Letts*. **302**, 113 (1999).
19. I. Wallace and W.H. Breckenridge, *J. Chem. Phys*. **98**, 2678 (1993).
20. D.J. Funk, A. Kvaran, and W.H. Breckenridge, *J. Chem. Phys*. **90**, 2915 (1989).
21. V.A. Bracken, P. Guertler, and J.G. McCaffrey, *J. Chem. Phys*. **107**, 5290 (1997).
22. D.V. O'Connor and D. Phillips, *Time Correlated Single Photon Counting*, Academic, London (1984).
23. ZFIT program for Nonlinear Least Squares Analysis of Fluorescence Decay Data by M. Rehorek, H. Otto, W. Rettig and A. Klock, and modified by P. Gürtler, and M. Joppien, last update August 1995.
24. The Gaussian functions used were of the form $G(x) = a \exp[-(x - m)^2/(2s^2)]$, where a, m and s represent the intensity, the position and the variance, respectively.
25. NIST Atomic Spectra Database (Ver. 4), available: http://www.nist.gov/pml/data/asd.cfm [2012, March] (National Institute of Standards and Technology, Gaithersburg, MD).
26. J.R. Fuhr and W.L. Wiese, *Handbook of Chemistry and Physics*, D.R. Lide (ed.), 73rd Edition (CRC, Boca Raton, 1991–1993).

27. The emission band in the upper panel has a larger bandwidth than that of the emission in the lower panel of Fig. 8 due to the fact it was scanned at a lower resolution.
28. Sites of cubic symmetry are created by placing the guest metal atom in single-vacancy (sv), tetra-vacancy (tv) or hexa-vacancy (hv) sites. The Io_h site is intrinsic to the close packed fcc lattice. It corresponds to the void between six atoms arranged as a triangle on one layer and an oppositely oriented triangle from an adjacent layer. A tv site is created by the removal of a tetrahedron of four adjacent host atoms surrounding a tetrahedral interstitial (I_{Td}) site in the fcc lattice. When the six atoms (described above) surrounding an Io_h site are removed, a hexa-vacancy is produced.
29. M.A. Ryan, M. Collier, P. dePujo, C. Crepin, and J.G. McCaffrey, *J. Phys*. *Chem.* **A114**, 3011 (2010).
30. P.N. Kerins and J.G. McCaffrey, *J. Chem. Phys*. **109**, 3131 (1998).
31. P. Kerins, B. Healy, and J.G. McCaffrey, *Fiz. Nizk. Temp*. **26**, 1016 (2000) [*Low Temp. Phys*. **26**, 756 (2000)].
32. The second emission band present at 470 nm in the Mg/Xe system corresponds to spin triplet emission.
33. R.A. Aziz and M.J. Slaman, *Chem. Phys*. **130**, 187 (1988).